Specific heat of quasi-crystals

Emília Illeková[1], Jean-Jacques Kuntz[2], Jean-Claude Gachon[2], Peter Šimon[3]

[1]Institue of Physics, Slovak Academy of Sciences, Dúbravská cesta 9, SK-842 28 Bratislava, Slovakia
[2]UMR 7555, Groupe Thermodynamique et Corrosion, Université Henri Poincaré, Nancy 1, BP 239, F-54506 Vandoeuvre-lès-Nancy, Cedex, France
Department of Physical Chemistry, Faculty of Chemical and Food Technology, SK-812 37 Bratislava, Slovakia
Email:fyziille@savba.sk, Jean-Claude.Gachon@lcsm.uhp-nancy.fr, simon@cvt.stuba.sk

Abstract

Molar heat capacity from 310 to 873 K has been determined for $Al_{94}Fe_2V_4$ ribbon. The classical integral step-by-step method and the dynamic mode differential scanning calorimetry method dates were mutually related. Specific heats of all Al-rich multicomponent nanostrustured systems, i.e containing amorphous, quasicrystalline or crystalline grains of nanometer dimensions, are anomalously low reflecting the presence of another Al-rich phase – the interphase.

Key words: heat capacity, differential scanning calorimetry, DSC, DDSC, aluminium base alloys, $Al_{94}Fe_2V_4$, quasicrystals

1 Introduction

This study is a part of the complex investigation of thermodynamic properties of Al-base alloys. Referring to previous two Seminars on Thermophysics, our attempt has concentrated into two principal levels: (1) the specific heat, $c_p(T)$, measurements at elevated temperatures T, and (2) the relation between the thermodynamic state of a sample and its $c_p(T)$. Thus, we have introduced the continuous mode differential scanning calorimetry (DSC) (Perkin-Elmer DSC7) in [1], the step-by-step DSC (Setaram111) in [2] and the drop calorimetry (Setaram2400) in [2]. In this paper, the dynamic differential scanning calorimetry (DDSC) (Perkin-Elmer DSC7) is tested. The $c_p(T)$ temperature dependence of $Al_{94}Fe_2V_4$ ribbon from 310 to 873 K is presented. The DDSC data are compared to the standard step-by-step DSC temperature dependence of the molar heat capacity of the ribbon sample.

Concerning the thermodynamics, $c_p(T)$ of various Al-based samples have already been characterized. First, the data for the standardized pure fcc-Al were attested and those for single phase compounds as Al_3Fe and Al_3Nb have been presented and analyzed in [2]. Further, the Neumann-Kopp rule for polycrystalline alloys (namely for $Al_{90}Fe_7Nb_3$) was reconfirmed while the thermal insufficiency of the same composition but nanocrystalline alloy was discovered in [3]. This lag in the bulk heat capacity is preserved and even increased after the melting of the Al-rich phase. The principal relation between the as-prepared amorphous, relaxed and crystallized states of the same sample has been quantitatively characterized for the first time in [1].

The nano-quasicrystalline $Al_{94}Fe_2V_4$ ribbons, which are the subject of this study, have been reported to exhibit both good bending ductility and tensile fracture strength [4]; however, neither their thermodynamic state nor their structure has been characterized yet. (Generally, the quasicrystalline structure has the icosahedral or decagonal symmetry. It is an ordered structure involving several extremely large structural units but it lacks the long-range periodicity. For example, the two structural units of the decagonal $Al_{70}Ni_{15}Co_{15}$ structure consist of 66 and 110 atoms, see Fig.1 [5]. The structural details in the icosahedral $Al_{94}Fe_2V_4$ might be more complicated.)
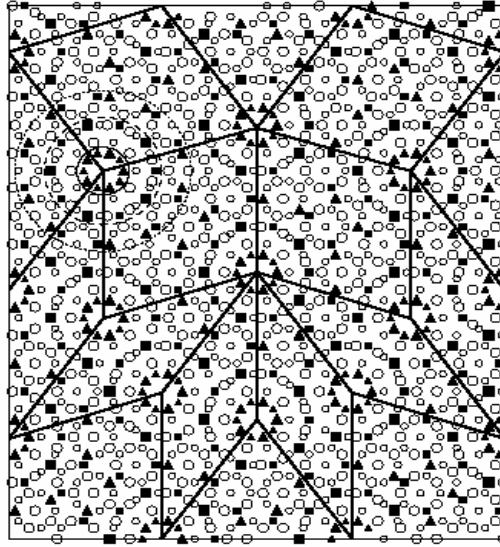

Fig 1 Projection of the 1276-atom large-rhombus-tiling model for d-AlNiCo onto the quasiperiodic plane. Open circles, Al atoms; filled triangles, Ni atoms; filled squares, Co atoms [5].

2 Experimental and results

2.1 Samples

The Al_{94} Fe_2V_4 ribbons (29 μm thick and 10 mm wide) were formed by planar flow casting of the melt at 1600 K at 10^6 K s^{-1} in air. The true chemical composition was checked by the inductively coupled plasma spectroscopy (±1 % of element content). X-ray diffraction analysis (CuK_α radiation) and transmission electron microscopy determined the existence of a mixed structure consisting of nanoscale icosahedral τ-phase (I) [4] (the particle size is ~ 80 nm) surrounded by the fcc-Al phase (~ 30 nm) and amorphous matrix (~ 30 vol. %) in the as-quenched samples. The particle size of both fcc-Al and I phases increased over 100 nm after additional crystallization and recrystallization at 773 - 873 K.

Classical continuous heating DSC (± 0.05 % for T and ± 2 % for the transformation enthalpy, H_{tr}) and DTA (differential thermal analysis, ±0.1 % for T, and ± 5 % for H_{tr}) was used to characterize the thermodynamic stability of the sample. Perkin-Elmer DSC-7 and Perkin-Elmer DTA-7 apparatuses, the heating rates 40 and 10 K min^{-1}, open Al and aluminum crucibles with lids, eventually, and both flowing argon and nitrogen atmospheres (30 ml min^{-1}) were used. Relating to the $Al_{90}Fe_7Nb_3$ ribbon in Fig. 2, the

DSC thermogram of $Al_{94}Fe_2V_4$ ribbon reveales the absence of amorphous Al and the stability of both nanocrystalline and icosahedral phases up to 783 K (at the heating rate +40 K min^{-1}). At higher temperatures, only one weak exothermal peak occurs having the onset temperature, T_{x1} = 802 K and H_{cr1} = -16 J g^{-1}. Besides, the DTA thermogram indicates at least two-step melting, namely the melting of the eutectics between the Al-rich solution at T_{m1} = 915 K and H_{m1} = 182 J g^{-1} and the aluminides of Fe and V at T_{m2} = 1040 K, H_{m2} = 46 J g^{-1}. The relation between H_{m1} and the enthalpy of melting of fcc-Al being $H_{m,Al}$ = 397 J g^{-1} [6] indicates that only 51.6 % of total Al (linking to 67.2 % in the case $Al_{90}Fe_7Nb_3$ ribbon) present in the alloy persists in the fcc-Al phase. A massive exotherm (-1424 J g^{-1}) refers to the reaction between the sample and its surroundings above 1300 K.

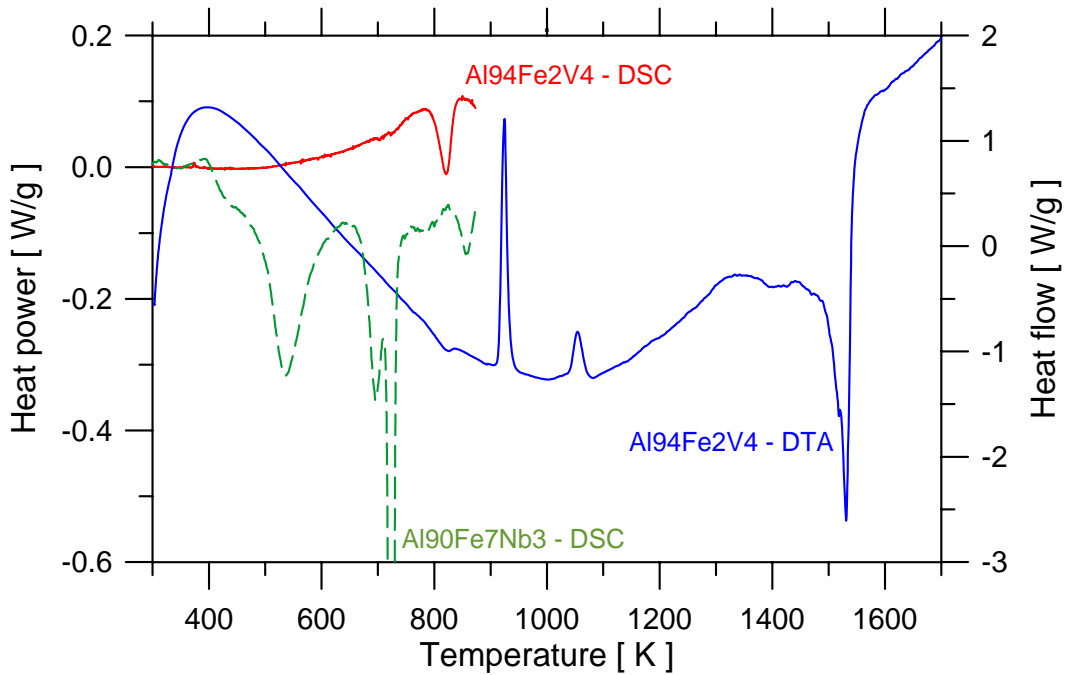Fig 2. DSC (heating rate 10 K min^{-1}) and DTA (10 K min^{-1}) curves for as-quenched $Al_{94}Fe_2V_4$ ribbon. For comparison is the DSC (40 K min^{-1}) dashed line for amorphous $Al_{90}Fe_7Nb_3$ ribbon [6].

2.2 Continuous mode differential scanning calorimetry: integral step-by-step method for heat capacity measurements

The molar heat capacity at constant pressure, Cp, (the reproducibility ±0.1 J mol^{-1} K^{-1}, the overall uncertainty ±5%) was determined with Setaram DSC-111, designed as a Calvet type calorimeter. The temperature between 310 and 1080 K was increased in 10 K steps. The heating rate was 3 K min^{-1} for 200 s and then the temperature was kept constant for 400 s, in each temperature step. So, while an overall heating rate was 1 K min^{-1}, the steady state in the sample could be realized in each temperature step (except the transformation regions giving the anomalous artifacts). The discrete values for $<Cp(T)>$ being the mean values in individual temperature steps were calculated by the numerical integration of the DSC signal. The sample of 0.135 g, alumina crucibles and an Ar atmosphere were used. The complete procedure has been described in [2].
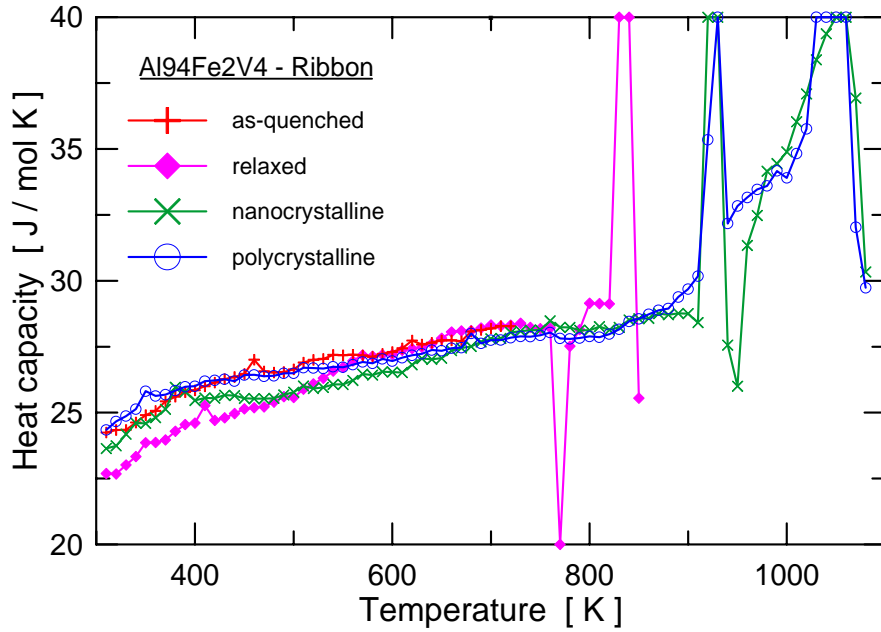
Fig 3. Temperature dependence of molar heat capacity of $Al_{94}V_2V_4$ ribbon. As-quenched ($+$), relaxed up to 720 K ($\blacklozenge$), after recrystallization up to 870 K ($\times$) and after melting by heating up to 1080 K sample ($\circ$). Zig-zag lines connect the experimental data.
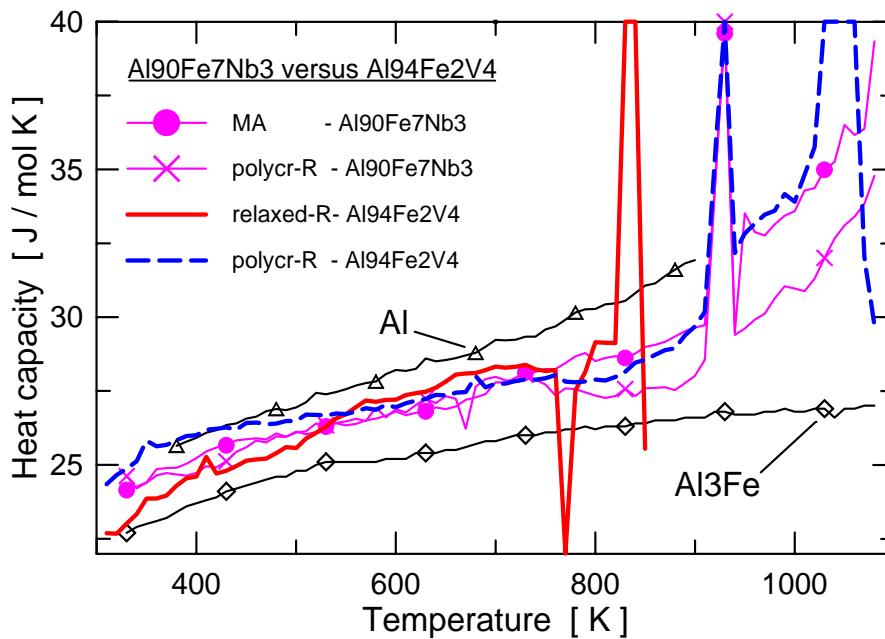

Fig 4. Experimental molar heat capacities (± 1 J mol^{-1} K^{-1}) of the bulk master alloy ($\bullet$) and polycrystalline ribbon ($\times$) of $Al_{90}Fe_7Nb_3$ alloy [3]; and quasicrystalline ribbon (—) and polycrystalline ribbon (— —) of $Al_{94}Fe_2V_4$ alloy. Data for fcc-Al (Δ) and Al_3Fe ($\Diamond$) phases [3] are shown as well. Zig-zag lines connect the experimental data. (Not all data points are shown.)

No appreciable oxidation, weight losses or reactions between samples and the alumina laboratory crucible were observed at the end of the measurements.

The $C_p(T)$ of the $Al_{94}Fe_2V_4$ sample (Fig.3) was measured in four subsequent heating cycles, where the thermodynamic state, namely the particular phases and their morphologies were modified by the gradual increase of the final temperature of each preceding heating cycle (see the legend to Fig. 3). First, both the absolute values and the shape of $C_p(T)$ dramatically change due to the structural relaxation at lower temperatures (in the first run). Then, the polynomial tendency of $C_p(T)$ gradually saturates to reach its final representative value, which for the quasicrystalline sample (in the second run) is

$$Cp(T) = 24.9 + 0.00428\ T + 2.29*10^{-6}\ T^2 - 152\ T^{-1} - 375000\ T^{-2} \tag{1}$$

and in the case of the polycrystalline sample (in the fourth run) is

$$Cp(T) = 25.9 + 0.00084\ T + 3.70*10^{-6}\ T^2 - 67.1\ T^{-1} - 140000\ T^{-2}. \tag{2}$$

The irregularities in the individual curves reflect the configurational contributions to $C_p(T)$ due to the recrystallization and coalescence effects in the second run and the two-step melting in the third run and the fourth run.

Fig. 4 shows that $C_p(T)$ for the $Al_{94}Fe_2V_4$ alloy in any sample state is within the corridor of the pure fcc-Al and monoclinic Al_3Fe components ones (while $C_p(T)$ for the vanadium containing phases is not yet known). However, the Neumann-Kopp rule valid in the conventional polycrystalline mixtures is hindered in the soft-grained structures. Whichever state, amorphous, quasicrystalline or crystalline, the elementary phase components are, the volume fraction of the interphase between them remains of the same order in the case of the nanodimensional grained structure [7] and thus its heat capacity contribution, $C_{p,\,interpase}(T)$, must always be significant. The heat capacity of fcc-Al, $C_{p,Al}(T)$, has extremely large anharmonic contributions [8]. Thus, specifically the overall $C_p(T)$ of each nanostructured Al-rich alloy (being a weighted sum of the partial capacities of all elementary phases) is extremely sensitive to the quantity and also the quality of the interphase. In the case of $Al_{94}Fe_2V_4$ ribbon, the $C_{p,quasicryst.}(T)$ of a quasicrystalline relaxed sample is minimal (within ~ 5 %) with relation to the other forms of the sample at temperatures around 400 K. At higher temperatures, the $C_{p,nanocryst.}(T)$ of each nanocrystalline form is insufficient (within ~ 6 %) relatively to the polycrystalline counterparts $C_{p,polycryst}$.

2.3 Dynamic differential scanning calorimetry

The principles of the DDSC method are outlined in [[9,10]. In the temperature-modulated methods, the common linear heating program is superimposed with a periodical dynamic temperature change (mostly sinusoidal, saw-tooth or step-wise). In DDSC, the treatment of heat flow is based on the linear response theory in which the analysis of the dynamic component yields a complex heat capacity with a real part (storage heat capacity) and an imaginary part (loss heat capacity). This complex heat capacity is dependent on the frequency of the temperature modulation. The real part of the heat capacity describes molecular motions and corresponds to the heat capacity in the case of equilibrium. The imaginary part is linked to dissipation processes.

The measurements were carried out using Perkin-Elmer DSC-7 calorimeter. The temperature regime was heat-cool, heating by 2 K, cooling by −1 K, heating rate ±3 K/min, so that the underlying heating rate was 1 K/min. The temperature range was 50–600 ^{o}C, purge gas was nitrogen. The temperature calibration was carried out using In, Sn and Zn, enthalpy calibration using In. The samples were placed in standard

aluminium pans with lids. The baseline subtraction was performed before the data treatment.

The DDSC method deduced storage molar heat capacity component, $C_{p,\cos}(T)$, for the as-quenched $Al_{94}Fe_2F_4$ ribbon sample (Fig. 6) follows the polynomial temperature dependence

$$C_{p,cos}(T) = 28.2 + 0.0177T - 1.24*10^{-6}T^2 , \tag{3}$$

with the ±0.25 J K^{-1} mol^{-1} noise. Besides the continuity of these data (related to the discrete points representing the individual mean values in the case of $C_p(T)$ determined by the step-by-step method) they do not include neither the excess heat capacity contributions of the not yet relaxed structure nor the configurational contributions during the phase transformations. It is also seen, that the change of the absolute value of $C_{p,\cos}(T)$ at the temperatures of the recrystallization of the sample due to this transformation is not significant in this case.
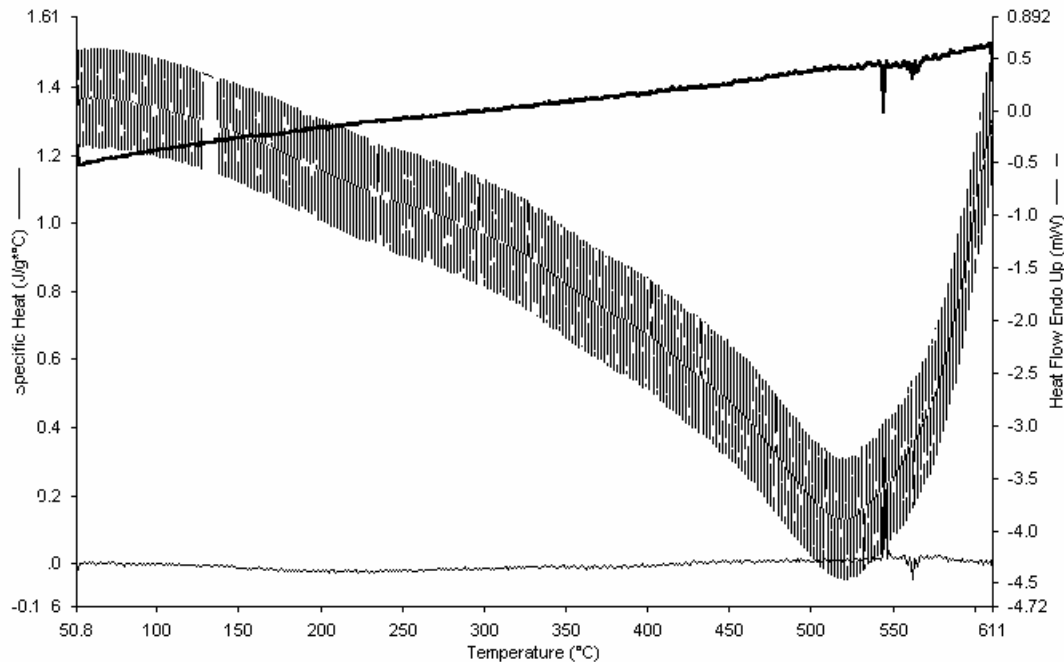

Fig 5. DDSC heat flow (the modulated curve), the loss heat capacity (the downward line) and the storage heat capacity (the upward line) for $Al_{94}Fe_2V_4$ as-quenched ribbon.

3 Discussion

The $C_{p,\cos}(T)$ curve for the as-quenched ribbon is approximately parallel to the $C_p(T)$ deduced by the step-by-step method for the relaxed sample (see Fig.6 or eqs. 1 and 3). The 45 % difference in the absolute values might reflect the systematical error of the DDSC data.

4 Conclusion

The as-quenched $Al_{94}Fe_2V_4$ ribbon contained besides the icosahedral τ-phase also the fcc-Al and Al-rich amorphous matrix, all of them in the form of nanometer size grains.

81

The molar heat capacity of both relaxed and recrystallized sample follows the polynomial temperature dependence in the range 310 – 873 K. The absolute values of $C_p(T)$ of all nanostructured forms of the sample, even after the remelting of the fcc-Al phase, was anomalously low reflecting the presence of another Al-rich phase – the interphase. Due to this interphase, the anomalous thermodynamic sequence, namely $C_{p,\text{polycryst.}} > C_{p,\text{nanocryst.}} > C_{p\text{quasicryst.}}$ would be expected in the case of all Al-rich multicomponent nanostrustured systems.

The DDSC (Perkin-Elmer) data were parallel but systematically higher by ~45 % than the step-by-step (Setaram) $C_p(T)$ due to the systematical error in the first method.
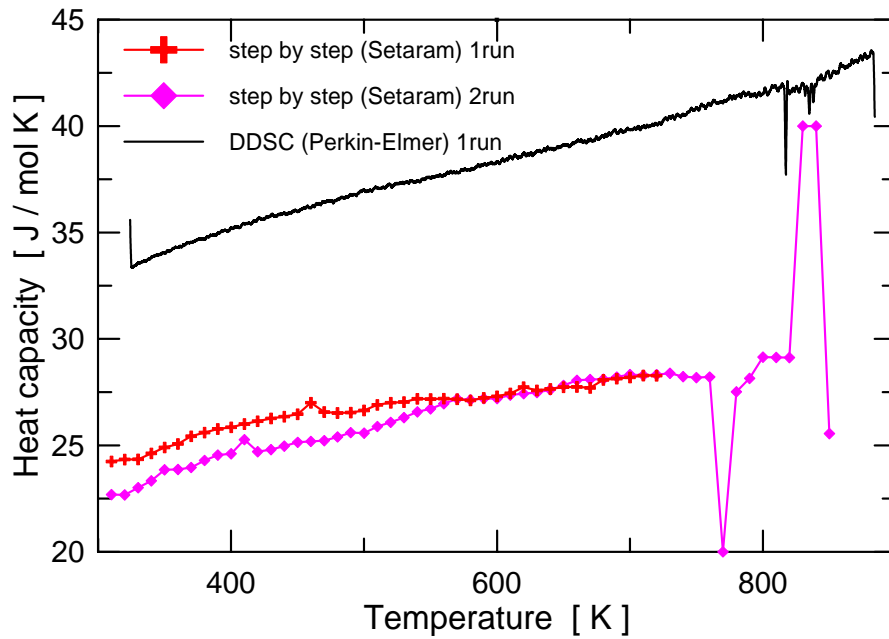

Fig 6. Relation between the step-by-step and DDSC experimental data for the $Al_{94}Fe_2V_4$ ribbon.

Acknowledgement

References

[1] Illeková E, Aba B, Kuhnast F A, 1992 Measurements of accurate specific heats of metallic glasses by differential scanning calorimetry (DSC). Part 1. Analysis of theoretical principles and accuracies of suggested measurement procedures, *Thermochim. Acta* **195** 195-209 and Illeková E, Aba B, Kuhnast F A, 1992 Measurements of accurate specific heats of metallic glasses by differential scanning calorimetry (DSC). Part 2. Specific heat of $Fe_{73}Co_{12}B_{15}$ metallic glass from 300 to 1054 K, *Thermochim. Acta* 211-220

[2] Illeková E, Gachon J C, Kuntz J J, Kuhnast F A, 2002 High temperature step by step calorimetry and drop caporimetry of metals, in *Thermophysics 2001. Meeting of the Thermophysical Society Working Group of the Slovak Physical Society, October 23-25, 2001*, (Ed. Vozár L, Nitra: Constantine the Philosopher University) pp.13-19

[3] Illeková E, Gachon J C, Kuntz J J, 2003 The validity of the Neumann-Kopp rule, in *Thermophysics 2002. Meeting of the Thermophysical Society Working Group of the Slovak Physical Society, October 24-25, 2002, Kočovce, Slovakia,* Ed.: Libor Vozár, Constantine the Philosopher University in Nitra Faculty of Natural Sciences 2003, pp. 71-76

[4] Inous A, Kimura H, Sasamori K, Masumot T, 1996 High mechanical strength of Al-(V,Cr,Mn)-(Fe,Co,Ni) quasicrystalline alloys prepared by rapid solidifcation, *Materials Transactions, JIM* **37** 1287-1292

[5] Krajčí M, Hafner J, Mihalkovič M, 2000 Atomic and electronic structure of decagonal Al-Ni-Co alloys and approximant phases, *Phys. Rev.* **B62** 243-255

[6] Illeková E, Švec P, 2002 Vznik a zánik nanokryštalického hliníka v zliatine $Al_{90}Fe_7Nb_3$, in *Proceedings of the 14th Conference of the Czech and Slovak Physicist, October 9–12, 2002, Plzeň,Czech Republik*, (Eds.: P. Baroch, M. Kubásek, Š. Potocký, Západočeská univerzita v Plzni 2002, 411-416

[7] Gleiter H 2000 Nanostructured materials: Basic concepts and microstructure, *Acta Mater.* **48** 1 - 29

[8] Barin I, 1993 *Thermochimical data of pure substances*, 2nd ed. Part 1, (Weinheim, Germany, VCH) p.17.

[9] Schawe J E K, 1995 Principles for the interpretation of modulated temperature DSC measurements. Part 1. Glass transition**,** *Thermochim.Acta* **261** 183-194

[10] Schawe J E K, 1995 A comparison of different evaluation methods in modulated temperature DSC, *Thermochim.Acta* **260** 1-16